

9-1973

A theoretical study of transient wave phenomena in gases

S E. Bonamy

R T. Wheway

Follow this and additional works at: <https://ro.uow.edu.au/wucbull>

Recommended Citation

Bonamy, S E. and Wheway, R T., "A theoretical study of transient wave phenomena in gases" (1973).
Wollongong University College Bulletin. 32.
<https://ro.uow.edu.au/wucbull/32>

Research Online is the open access institutional repository for the University of Wollongong. For further information contact the UOW Library: research-pubs@uow.edu.au

A theoretical study of transient wave phenomena in gases

WOLLONGONG UNIVERSITY COLLEGE
THE UNIVERSITY OF NEW SOUTH WALES



A THEORETICAL STUDY OF
TRANSIENT WAVE PHENOMENA
IN GASES

S. E. BONAMY

and

R. T. WHEWAY

DEPARTMENT OF THERMAL ENGINEERING

September, 1973

A THEORETICAL STUDY OF TRANSIENT
WAVE PHENOMENA IN GASES

S. E. BONAMY

and

R. T. WHEWAY

CONTENTS

	<u>Page</u>
Introduction	1
List of Symbols	2
Basic Equations	5
Computation Techniques for Network	10
References	18
Figures	19

Introduction

The application of the method of characteristics provides a useful method for a study of wave phenomena following the sudden release of gas in a tube. To obtain sufficient accuracy when using this technique, it is necessary to calculate values along the various characteristics on a position diagram rather than use the more conventional graphical method employing an auxiliary state diagram. The step by step processes of calculating values, and determining resulting pressure vs time and pressure vs distance diagrams, is best done with the aid of a high speed digital computer. Storage within the computer eliminates the need to actually plot a position diagram, although such a plot is useful for a physical understanding of the problem.

The effect of wall friction and heat transfer on the propagation of waves in a mechanical shock tube has been studied by Bannister (Ref. 1) and Bonamy (Ref. 2). The resulting partial differential equations describing the flow were solved by both these authors using the method of characteristics, but the numerical method of integration required along the characteristics for accurate plotting of the position diagram limited the work to the study of one pressure ratio only. This work was extended by Bonamy and Wheway (Ref. 3) by introducing computer programmes, which not only solved the network for any number of pressure ratios, but also provided a direct read-out of pressure and/or temperature vs time and distance histories. Comparison of these theoretical values with those obtained by experiment permitted an examination of the effects of heat transfer across the contact surface, or gaseous interface which is formed on the initiation of the shock and separates the "shocked" and "rarefied" gas. Insufficient information concerning boundary conditions prevented the inclusion in the theory of heat and mass transfer effects across the contact surface.

The present paper is an expansion of the latter work describing in more detail the development of the characteristic equations and the

programming procedure used for their solution.

LIST OF SYMBOLS

$$A = w_+ + S_+ y_+$$

$$\bar{A} = \bar{w}_+ + R \bar{S}_+ \bar{y}_+$$

$$a = \text{acoustic velocity}$$

$$\bar{a}_O = \text{local acoustic velocity if gas were brought isentropically from } P \text{ to } P'_O$$

$$B = w_- - S_- y_-$$

$$\bar{B} = \bar{w}_- - R \bar{S}_- \bar{y}_-$$

$$C = \left(-w_+ + \beta_+ \right) \alpha_+$$

$$D = \text{pipe diameter}$$

$$E = \text{internal energy}$$

$$F = \text{body force}$$

$$F_f = \text{friction force at wall}$$

$$f = \text{steady state friction factor}$$

$$G = \left(-w_- - \beta_- \right) \alpha_-$$

$$\bar{G} = \left(-\bar{w}_- - \bar{\sigma}_- \right) \bar{\alpha}_- R^{0.788}$$

$$H = \frac{\beta_* \alpha_*}{2 y_*}$$

$$h = \text{convection heat transfer coefficient}$$

$$K = \frac{f}{2 D}$$

$$k = \text{thermal conductivity coefficient}$$

$$\bar{L} = \sqrt{\frac{6R^7 (\bar{y})^7 + 1}{7}}$$

$$\bar{M} = \frac{5 [(\bar{L})^2 + 1] R^7 (\bar{y})^6}{2(\bar{L})^3}$$

P = absolute pressure

Q = heat added

$$R = \left(\frac{P'_0}{P''_0} \right)^{\frac{\gamma-1}{2\gamma}} = \left(\frac{P'_0}{P''_0} \right)^{\frac{1}{7}} \text{ based on } \gamma = 1.40$$

$$S = \frac{\bar{a}_0}{a'_0}$$

T = absolute temperature

t = time

U = potential energy

u = directional velocity component

V = total velocity

$$w = \frac{u}{a'_0}$$

x = distance

$$y = \left(\frac{P}{P'_0} \right)^{\frac{\gamma-1}{2\gamma}} = \left(\frac{P}{P'_0} \right)^{\frac{1}{7}} \text{ based on } \gamma = 1.40$$

$$\alpha = \frac{(S|w|)^{0.786}}{y^{0.711}}$$

$$\beta = 1.090 \left(\frac{1}{Sy} - Sy \right) + \frac{2w^2}{5Sy}$$

γ = ratio of specific heats

δ = unit vector

θ = temperature difference between gas and tube

μ = absolute viscosity

π_{ji} = stress tensor

ρ = density

$$\sigma = 1.090 \left(\frac{1}{SRy} - SRy \right) + \frac{2w^2}{5SRy}$$

τ_{ij} = shear stress

$$\gamma = \left\{ \frac{0.3409 (T'_o)^{0.787}}{D^{1.214} (P'_o)^{0.214}} \right\} t$$

$$x = \left\{ \frac{0.006969 (T'_o)^{0.287}}{D^{1.214} (P'_o)^{0.214}} \right\} x$$

Subscripts

i, j, k co-ordinate directions

o initial state

s shock

+, -, * characteristics

~ vector

Superscripts

' gas initially in high pressure region

" gas initially in low pressure region

- "shocked" gas between contact surface and shock front

BASIC EQUATIONS

The bursting of a membrane initially separating a high and low pressure gas in a tube causes the propagation of a shock wave into the low pressure region and a rarefaction wave into the high pressure region. The contact surface, which is a discontinuity in temperature and density is propagated in the same direction as the shock wave. A boundary layer develops between the head of the rarefaction wave and the shock front as shown in Fig. 1.

Considering an elemental volume of this gas at time t , Fig. 2, continuity, momentum and energy equations can be established as follows :

Continuity

A well known form of the continuity equation (Ref. 4) is

$$\frac{d\rho}{dt} + \rho \operatorname{div} \underline{v} = 0.$$

Using repeated suffix notation, this may be modified to

$$\frac{\partial \rho}{\partial t} + \left(u_i \frac{\partial \rho}{\partial x_i} + \rho \frac{\partial u_i}{\partial x_i} \right) = 0 \quad \dots (1)$$

Momentum

Following a similar technique to that for the continuity equation it can be shown (Ref. 4) that the resultant force acting on unit volume of fluid due to normal and shear stresses is given by

$$\delta_i \frac{\partial \pi_{ji}}{\partial x_i}$$

$$\text{Now } \pi_{ji} = -P \delta_{ij} + \mu \left(\frac{\partial u_i}{\partial x_j} + \frac{\partial u_j}{\partial x_i} \right)$$

Applying Stokes' assumptions,

$$\pi_{ji} = -P \delta_{ij} + \tau_{ij} - \frac{2}{3} \mu \frac{\partial u_k}{\partial x_k} \delta_{ij}$$

Equating the resultant force to the rate of change of momentum gives

$$\delta_i \rho F_i + \delta_i \frac{\partial \pi_{ji}}{\partial x_j} = \rho \delta_i \left(\frac{\partial u_i}{\partial t} + u_j \frac{\partial u_i}{\partial x_j} \right) \dots (2)$$

Energy

The "total energy equation" may be written (Ref. 4) as

$$\begin{aligned} \frac{\partial}{\partial t} (E) + \frac{\partial}{\partial x_i} (E u_i) + \frac{d}{dt} \left(U + \frac{V^2}{2} \right) &= \frac{\partial U}{\partial t} + Q + \frac{1}{\rho} \operatorname{div} (k \operatorname{grad} T) - \\ &- \frac{1}{\rho} \operatorname{div} (FV) + \frac{1}{\rho} \nabla \cdot (\tau_{ij} \delta_i \delta_j \cdot \underline{V}) - \frac{2}{3\rho} \underline{V} \cdot \operatorname{grad} (\mu \operatorname{div} \underline{V}) \end{aligned} \dots (3)$$

In equation (3) the term

$$\frac{1}{\rho} \operatorname{div} (k \operatorname{grad} T) = \text{heat loss by conduction ;}$$

$$\frac{1}{\rho} \operatorname{div} (FV) = \text{work done by pressure forces ;}$$

$$\frac{1}{\rho} \nabla \cdot (\tau_{ij} \delta_i \delta_j \cdot \underline{V}) = \text{work done by shear stresses; and}$$

$$\frac{2}{3\rho} \underline{V} \cdot \operatorname{grad} (\mu \operatorname{div} \underline{V}) = \text{work done by dilation.}$$

Equations (1), (2) and (3) apply to the general case where the flow comprises both a volume of fluid with constant property values across the core and the boundary layer where properties vary from freestream values to those at the wall. Their solution is prevented by the lack of knowledge of the non-steady boundary layer and of the nature of heat and mass transfer across the contact surface. However, it has been found that for tubes of 2 inches diameter and larger (Refs. 1 and 3), the volume of the tube occupied by the boundary layer is insignificant.

The fluid properties can therefore be treated as uniform across the tube and the problem is reduced to one in which the flow is one-dimensional. The effects of the velocity boundary layer and the thermal boundary layer may then be isolated to the tube wall as a frictional force opposite in direction to the flow and a flow of heat into or out of the fluid.

Using these assumptions and considering the contact surface as a plane discontinuity in density and temperature across which there is no flow of heat, equations (1), (2) and (3) may be modified as follows.

Continuity

$$\frac{\partial \rho}{\partial t} + \rho \frac{\partial u}{\partial x} + u \frac{\partial \rho}{\partial x} = 0. \quad \dots (4)$$

Momentum

After expanding and neglecting second order terms, equation (2) becomes

$$-\rho F + \frac{\partial P}{\partial x} + \rho \frac{\partial u}{\partial t} + \rho u \frac{\partial u}{\partial x} = 0.$$

Considering the whole tube

$$F_f + \int_{\text{vol.}} -\rho F + \int_{\text{vol.}} \frac{\partial P}{\partial x} + \int_{\text{vol.}} \rho \frac{\partial u}{\partial t} + \int_{\text{vol.}} \rho u \frac{\partial u}{\partial x} = 0,$$

where F_f , the frictional force at wall = area x shear stress

$$= (\pi D dx) \cdot f \frac{u^2 \rho}{g}$$

$$= \left(\frac{\pi D^2}{4} dx \right) \cdot K u^2 \rho$$

Now as the body force is zero, $\int_{\text{vol.}} -\rho F = 0.$

$$\therefore Ku^2 \rho \left(\frac{\pi D^2}{4} dx \right) + \frac{\partial P}{\partial x} \left(\frac{\pi D^2}{4} dx \right) + \rho \frac{\partial u}{\partial t} \left(\frac{\pi D^2}{4} dx \right) + \rho u \frac{\partial u}{\partial x} \left(\frac{\pi D^2}{4} dx \right) = 0.$$

$$\text{i.e. } \frac{\partial P}{\partial x} + Ku^2 \rho + \rho \frac{\partial u}{\partial t} + \rho u \frac{\partial u}{\partial x} = 0 \quad \dots (5)$$

Energy

Referring to equation (3) the terms $\underline{V} \cdot \text{grad div } \underline{V}$, $(\underline{V} \cdot \text{grad } \mu)$ $(\text{div } \underline{V})$ and $\frac{1}{\rho} \text{div} (k \text{ grad } T)$ are second order terms and may be neglected.

Also the term $\frac{1}{\rho} \nabla \cdot \left(\tau_{ij} \delta_i \delta_j \cdot \underline{V} \right) = 0$ for one dimensional flow.

Therefore equation (3) becomes

$$\rho \frac{d}{dt} \left[E + U + \frac{V^2}{2} \right] + \rho E \frac{\partial u}{\partial x} = \rho \frac{\partial U}{\partial t} + \rho Q - \text{div} (P\underline{V}) .$$

Since $F = 0$ and $U = 0$, this reduces to

$$\left(\frac{\gamma}{\gamma-1} P + \rho u^2 \right) \frac{\partial u}{\partial x} + \rho u \frac{\partial u}{\partial t} + \frac{\gamma}{\gamma-1} u \frac{\partial P}{\partial x} + \frac{1}{\gamma-1} \frac{\partial P}{\partial t} + \rho Q = 0.$$

Considering now a whole tube of thickness dx and isolating heat addition to the tube wall such that $Q_w = h\theta (\pi D dx)$

$$\left(\frac{\gamma}{\gamma-1} P + \rho u^2 \right) \frac{\partial u}{\partial x} + \rho u \frac{\partial u}{\partial t} + \frac{\gamma}{\gamma-1} u \frac{\partial P}{\partial x} + \frac{1}{\gamma-1} \frac{\partial P}{\partial t} + \frac{4h\theta}{D} = 0 \quad (6)$$

The only known boundary conditions for the solution of equations (4), (5) and (6) are those at time, $t = 0$ and those along the rarefaction wave-front where the velocity is equal to the local sonic velocity. Thus solution by finite difference methods is not possible and the problem lends itself to the application of the method of characteristics.

Expressions for the three characteristic directions on a position diagram may be obtained and corresponding equations for finite differences in other properties along these characteristics developed from equations (4), (5) and (6). These are then transformed into a dimensionless form (Ref. 3) and extended to include the steady state values for the friction factor (Ref. 5) and the heat transfer coefficient (Ref. 6).

Finally, in order to obtain a characteristic network which is independent of tube diameter, initial pressure and temperature, two dimensionless parameters τ and X are introduced as co-ordinates of the position diagram.

The characteristics on the τ vs X plane are then represented by the following pairs of equations; the first of each pair gives the slope of the characteristic and the second relates changes in properties along that characteristic. The characteristic equations and resulting curves are identified as C_+ , C_- , and C_* , the C_+ and C_- corresponding to the propagation of points on rightward and leftward moving waves and the C_* to the movement of a gas particle. Two sets of equations are used depending on the initial state of the gas.

Gas initially in High Pressure Region

$$C_+ \text{ characteristic } \left\{ \begin{array}{l} \left(\frac{dX}{d\tau} \right)_+ = w + Sy \quad \dots (7a) \end{array} \right.$$

$$dw_+ = -5 S dy_+ + (\beta - w) \alpha d\tau_+ \quad \dots (7b)$$

$$C_- \text{ characteristic } \left\{ \begin{array}{l} \left(\frac{dX}{d\tau} \right)_- = w - Sy \quad \dots (8a) \end{array} \right.$$

$$dw_- = 5 S dy_- - (\beta + w) \alpha d\tau_- \quad \dots (8b)$$

$$C_* \text{ characteristic} \left\{ \begin{array}{l} \left(\frac{dX}{d\tau} \right)_* = w \quad \dots (9a) \\ dS_* = \frac{\beta \alpha}{2\gamma} d\tau_* \quad \dots (9b) \end{array} \right.$$

Gas initially in Low Pressure Region

$$C_+ \text{ characteristic} \left\{ \begin{array}{l} \left(\frac{dX}{d\tau} \right)_+ = w + SR\gamma \quad \dots (10a) \\ dw_+ = -5 SRdy_+ + (\sigma - w)\alpha (R)^{0.788} d\tau_+ \quad \dots (10b) \end{array} \right.$$

$$C_- \text{ characteristic} \left\{ \begin{array}{l} \left(\frac{dX}{d\tau} \right)_- = w - SR\gamma \quad \dots (11a) \\ dw_- = 5 SRdy_- - (\sigma + w)\alpha (R)^{0.788} d\tau_- \quad \dots (11b) \end{array} \right.$$

$$C_* \text{ characteristic} \left\{ \begin{array}{l} \left(\frac{dX}{d\tau} \right)_* = w \quad \dots (12a) \\ dS_* = \frac{\alpha \sigma}{2\gamma} \frac{1}{R^{0.212}} d\tau_* \quad \dots (12b) \end{array} \right.$$

$$\text{Shock-front (Ref. 7)} \left\{ \begin{array}{l} \left(\frac{dX}{d\tau} \right)_s = -\bar{L} \quad \dots (13a) \\ dw_s = -\bar{M} dy_s \quad \dots (13b) \end{array} \right.$$

COMPUTATION TECHNIQUES FOR NETWORK

In order to compute a network a step by step integration of equations (9) - (13) is necessary. As a result of this, the various characteristic curves take on shapes as shown in Fig. 3 (from Ref. 3),

which is a position diagram for an initial pressure ratio of 4.00 to 1. The diagram is seen to be developed from a series of triangular and quadrilateral elements; the general procedure involved is as follows.

1. Elements on Rarefaction Wave

Consider a typical quadrilateral element bounded by C_+ and C_- characteristics and intersected by a C_* characteristic as shown in Fig. 4. The problem is one of determining values of X and τ at the unknown points $B(I+1)$ and $D(I+1)$, values at other points being known from previous calculations. These must be found from the slopes of the various characteristics passing through the known points. The slopes depend upon average values of y , w , S along each line so that approximations of these at the unknown points $B(I+1)$ and $D(I+1)$ must first be made to obtain the average values. Successive calculations are then made using equations (7) to (9) until the desired accuracy is obtained.

From the geometry of Fig. 4 points $B_{(I+1)}$ and $D_{(I+1)}$ can be located from calculation of the finite increments $d\tau_+$, dX_+ , $d\tau_*$ and dX_* . These in turn are dependent on y , w and S so that increments in these quantities must be calculated concurrently. Simultaneous solution of expressions for $d\tau_+ - d\tau_-$ and $dX_+ - dX_-$ from equations (7a) and (8a) gives

$$d\tau_+ = \frac{\left(\frac{X_{A(I+1)} - X_{B(I)}}{A - B} \right) - B \left(\frac{\tau_{A(I+1)} - \tau_{B(I)}}{A - B} \right)}{A - B} \dots (14)$$

$$dX_+ = A d\tau_+ \dots (15)$$

Similarly from equations (7b) and (8b)

$$dy_+ = \frac{5 S_- \left(\frac{y_{A(I+1)} - y_{B(I)}}{5(S_+ + S_-)} \right) + \left(\frac{w_{A(I+1)} - w_{B(I)}}{5(S_+ + S_-)} \right) + \frac{Cd\tau_+ - Gd\tau_-}{5(S_+ + S_-)}}{5(S_+ + S_-)} \dots (16)$$

$$dw_+ = -5 S_+ dy_+ + Cd\tau_+ . \quad \dots (17)$$

Rewriting equation (9b)

$$dS_* = H d\tau_* . \quad \dots (18)$$

Also assuming a linear relationship along the C_+ characteristic so that, for example,

$$\frac{\tau_{D(I+1)} - \tau_{B(I)}}{\tau_{B(I+1)} - \tau_{B(I)}} = \frac{S_{D(I+1)} - S_{B(I)}}{S_{B(I+1)} - S_{B(I)}} . \quad \dots (19)$$

Computer programmes may be written to solve equations (14) to (19), incorporating an iteration procedure to obtain a desired accuracy of averaging values of the variables along each characteristic and then by using equations such as

$$\tau_{B(I+1)} = \tau_B + d\tau_+$$

values of τ , χ , y , w and S at the various points of the network for the gas initially in the high pressure region can be obtained.

In starting the network off at the origin of Fig. 3 points A(I) and B(I), Fig. 4, are coincident and the element is triangular. Since heat transfer and friction effects have not taken place at the origin, a range of values of y and w can be calculated assuming a frictionless adiabatic process. The most suitable range is for equal increments of y and w between the head and tail of the rarefaction wave corresponding to values on the fan-shaped C_+ characteristics at the origin. There is no movement of the gas along the head of the rarefaction wave, so that $y = 1$, $w = 0$ and $S = 1$ along this line. By choosing equal scales for τ and χ the rarefaction wave front SM' becomes a sloping line inclined at 45° to the τ and χ axes. An arbitrary increment is chosen along the χ axis for location of starting points for the C_- and C_* characteristics.

2. Elements on Compression Wave

The compression wave, bounded by the shock front and the contact surface, applies to the gas initially in the low pressure region. To complete this region of the network, it is necessary to link up equations applying to either side of the contact surface so that the elements are best considered in strips bounded by two C_+ characteristics. Beginning at the origin, the corner element is made up of two triangular elements separated by the contact surface as shown in Fig. 5. Symbols applying to the gas initially in the low pressure region are "barred" to distinguish them from those applying to gas initially in the high pressure region. The C_* and the \bar{C}_* characteristics are really coincident but are drawn as shown to facilitate examination of the elements. Conditions are the same along the two characteristics with the exception of S ; the formation of the shock causes a change in entropy and therefore the parameter S on the "shocked" side of the discontinuity whereas the formation of the rarefaction wave is initially an isentropic process. Further changes in S occur on both sides of the discontinuity as the waves progress due to friction and heat transfer effects.

To solve the element it is necessary to locate the unknown points $B(I)$, $B(I+1)$ and E , conditions at point $A(I+1)$ having been found from previous computations. The location is found from the slope of the various characteristics which again are dependent on average values of y , w and S along each line so that a trial-and-error approach must be made. Further, different equations apply to the characteristics on either side of the discontinuity requiring simultaneous solution, and since the path of the shock-front is not a characteristic different equations will apply to it also.

From the geometry of Fig. 5, simultaneous solution of expressions for $d\bar{\chi}_+$ + $d\bar{\chi}_-$ from equations (7a), (8a) and (9a) gives

$$d\tau_* = \frac{\left(\begin{matrix} X_{A(I+1)} - X_{A(I)} \\ w_* - B \end{matrix} \right) - B \left(\begin{matrix} \tau_{A(I+1)} - \tau_{A(I)} \end{matrix} \right)}{w_* - B} \quad . \quad (20)$$

$$dX_* = w_* d\tau_* \quad . \quad . \quad . \quad (21)$$

Also since $d\bar{X}_* = d\bar{X}_s + d\bar{X}_+$ from Fig. 5, a combination of equations (10a), (12a) and (13a) gives

$$d\bar{\tau}_s = \left(\frac{\bar{A} - \bar{w}_*}{\bar{A} + \bar{L}} \right) d\bar{\tau}_* \quad . \quad . \quad . \quad (22)$$

$$d\bar{X}_s = -\bar{L} d\bar{\tau}_s \quad . \quad . \quad . \quad (23)$$

Denoting $A(I)E$ on the \bar{C}_* characteristic by the subscript "o", $d\bar{X}_s = d\bar{X}_o + d\bar{X}_-$, so that from equations (11a), (12a) and (13a),

$$d\bar{\tau}_o = \frac{\bar{B} + \bar{L}}{\bar{B} - \bar{w}_o} d\bar{\tau}_s \quad . \quad . \quad . \quad (24)$$

$$d\bar{X}_o = \bar{w}_o d\bar{\tau}_o \quad . \quad . \quad . \quad (25)$$

The unknown points $B(I)$, $B(I+1)$ and E may be determined to a first approximation from Equations (20) to (25) by assuming the average slopes of the various characteristics and the shock front to be the same as at the known points. Noting that the dimensionless parameters X , τ , y and w have the same values on either side of the contact surface along the C_* characteristic, a geometrical consideration of Fig. 5 and a combination of equations (7b), (8b), (9b), (10b), (11b), (12b) and (13b) allows the changes in y , w and S along the characteristics and shock front to be computed; a linear variation along the C_* characteristic is assumed so that a proportionality constant can be introduced for determination of values at point E . More accurate values can then be used for the slopes of lines and location of unknown points. The complete process is repeated until

the desired accuracy is attained.

Proceeding to the left of the corner element, the next strip is as shown in Fig. 6. This is made up of two \bar{C}_+ characteristics, two \bar{C}_- characteristics, and two \bar{C}_* characteristics, together with the shock-front on one side of the contact surface and a C_+ , C_- , and C_* characteristic on the other. The additional \bar{C}_* characteristic represents the path of a gas particle originating from the shock-front at an arbitrarily chosen point. It is necessary to determine values of χ , τ , w and S at each of the points $B(I-1)$, $B(I)$, $B(I+1)$, E and $F(I)$, conditions at other points being known from previous computations. Thus simultaneous solution of equations as for the corner element, together with those for additional characteristics and consideration of the geometry of the figure enables computation of the unknown conditions for progression to the next strip.

The general strip between the shock front and contact surface is shown in Fig. 7. A detailed analysis of this strip has been considered by Wheway (Ref. 8).

3. Programmes developed for Network Analysis

In all, seven (7) computer programmes have been written to produce the characteristic network for any desired pressure ratio. A brief description of each of these programmes is given in the table below.

Programme	Function
1	solves typical element between the head of the rarefaction wave and contact surface (Fig. 4.).
2	calculates the initial equalisation pressure and values of the five dimensionless parameters at the starting point of the C_+ characteristics on the rarefaction wave-front.
3	solves 16 elements (all of which are similar to Fig. 4) between the head of the rarefaction wave and the contact surface.
4	solves corner element (Fig. 5) between the shock front and the contact surface.

Programme	Function
5	solves column 2 (Fig. 6) between the shock front and the contact surface.
6	solves column 3 onwards (between the shock front and the contact surface (such a column is shown in Fig. 7)).
7	used with programme 6 to solve a column in which a gas particle has overrun the shock front (see Fig. 8).

A more complete description and listings of both the programmes and samples of their output have been given by Wheway (Ref. 8).

An appreciation of the procedure adopted for calculating the network and the use of each of the programmes can be gained from an examination of Fig. 9. The computation procedure shown diagrammatically is by no means the only one possible and minor modifications may be introduced. However, experience in calculating the network for the four pressure ratios considered by the authors has shown that the procedure is the most convenient and results in the most efficient computer usage.

Pressure and particle velocity variations with time and distance.

For any particular combination of pressure and temperature of the gas initially in the high pressure region and tube diameter, the parameters τ and X are directly proportional to time and distance. Thus for a fixed distance along the X axis on the position diagram of Fig. 3 a vertical line intersecting the network would enable values of τ and, by interpolation, corresponding values of the dimensionless parameters and w to be computed. From these pressure and particle velocity variations with time at a fixed location in the tube are obtained. A horizontal line through the network shown in Fig. 3 allows similar computations against distance at a fixed interval of time. Pressure vs time and distance diagrams obtained in this manner,

together with others for gas temperature variations have been illustrated by the authors in Ref. 3.

Three (3) computer programmes have been developed for the determination of the pressure and particle velocity histories outlined above. Listings of these programmes, together with sample output are given in Ref. 8.

As stated earlier the programmes developed eliminate completely the necessity of plotting positions diagrams, so that pressure and/or particle velocity variations with time or distance can be obtained in a minimum of time. Modifications to the parameters χ and τ enable the programmes to be used for any initial pressure ratio, initial temperature or tube diameter. For the 2-inch diameter shock tube used in the present work it was reasonable to assume that boundary layer growth was insignificant. Discretion must be used when applying this theory to tubes of smaller diameter.

REFERENCES

1. BANNISTER, F.K. - Influence of Pipe Friction and Heat Transfer on Pressure Waves in Gases : Effects in a Shock Tube. Jour. Mech. Engg. Science, Vol. 6, No. 3, September, 1964, pp. 278-292.
2. BONAMY, S.E. - Pressure Wave Phenomena in a Uniform Shock Tube. Wollongong University College, Bulletin No. 6, April, 1964.
3. BONAMY, S.E. and WHEWAY, R.T. - The Transfer of Heat across a Gaseous Interface during the Propagation of a Shock Wave in a Tube. Mech. and Chem. Trans. I.E. Aust., Vol. MC6, No. 1, May, 1970, pp. 7-14.
4. WHITAKER, S. - Introduction to Fluid Mechanics. Prentice-Hall, 1968.
5. MOODY, L.F. - Friction Factors for Pipe Flow. Trans. ASME. Vol. 66, 1944.
6. CHAPMAN, A.J. - Heat Transfer. Macmillan, 2nd ed., 1967.
7. BANNISTER, F.K. and MUCKLOW, G.F. - Wave Action Following Sudden Release of Compressed Gas from a Cylinder. The Institution of Mechanical Engineers, Proceedings 1948, Vol. 159, pp. 269-300.
8. WHEWAY, R.T. - A Study of Wave Propagation in a Mechanical Shock Tube, Vol. 2. Unpublished Thesis, The University of New South Wales, 1967.

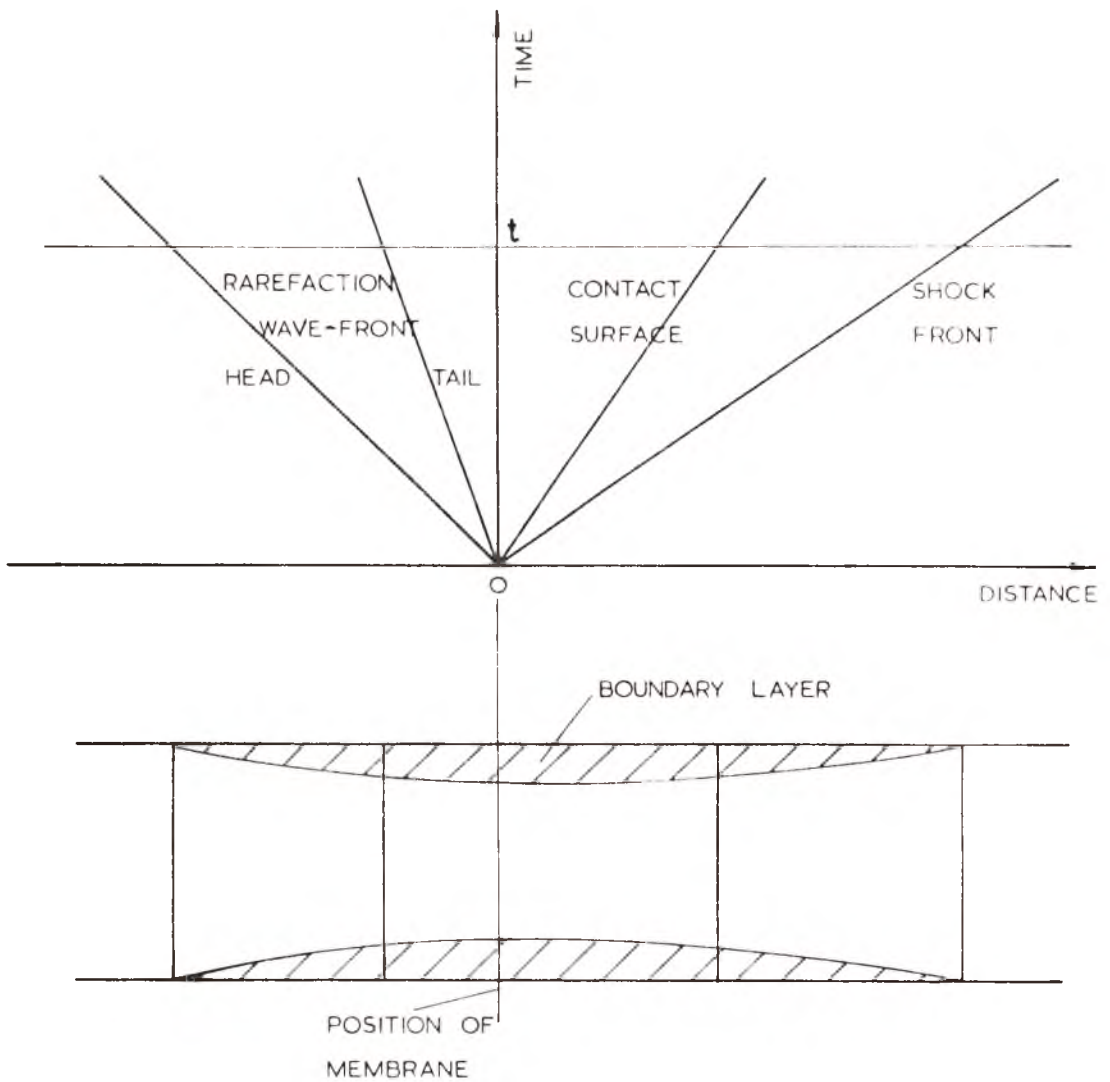


FIG.1.—Boundary Layer Growth in a Shock Tube at Time = t .

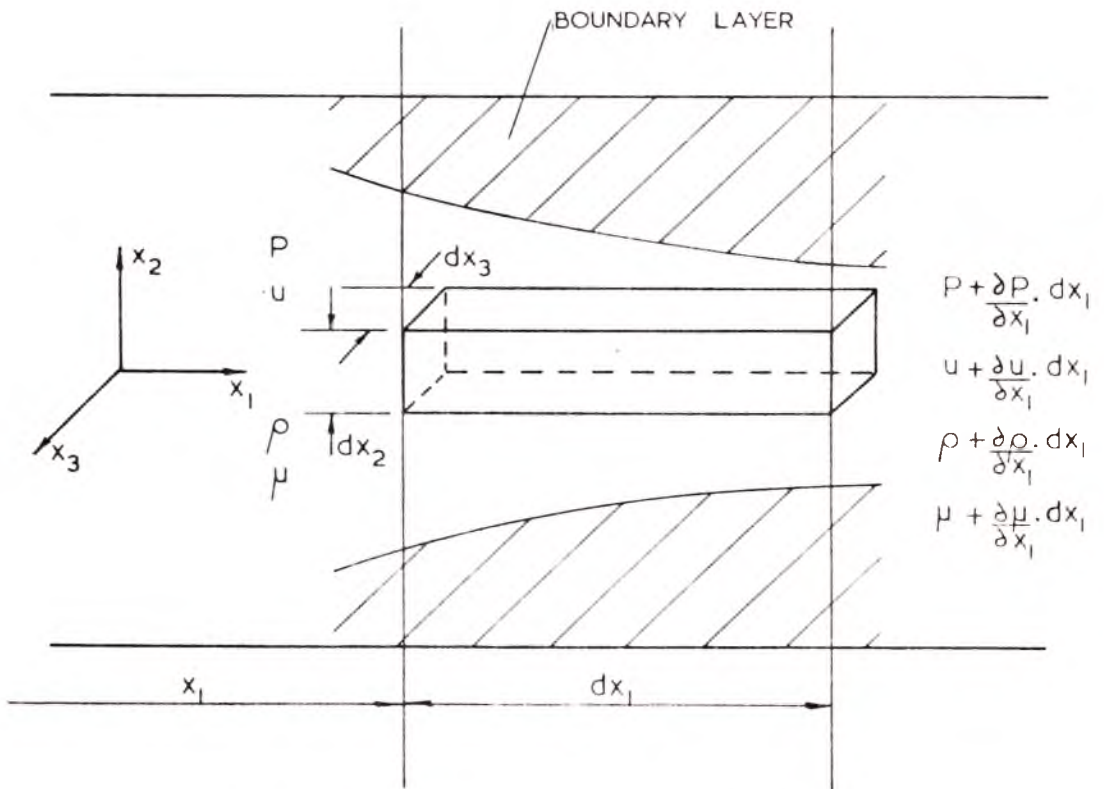


FIG. 2.—Elemental Volume in a Shock Tube at Time = t .

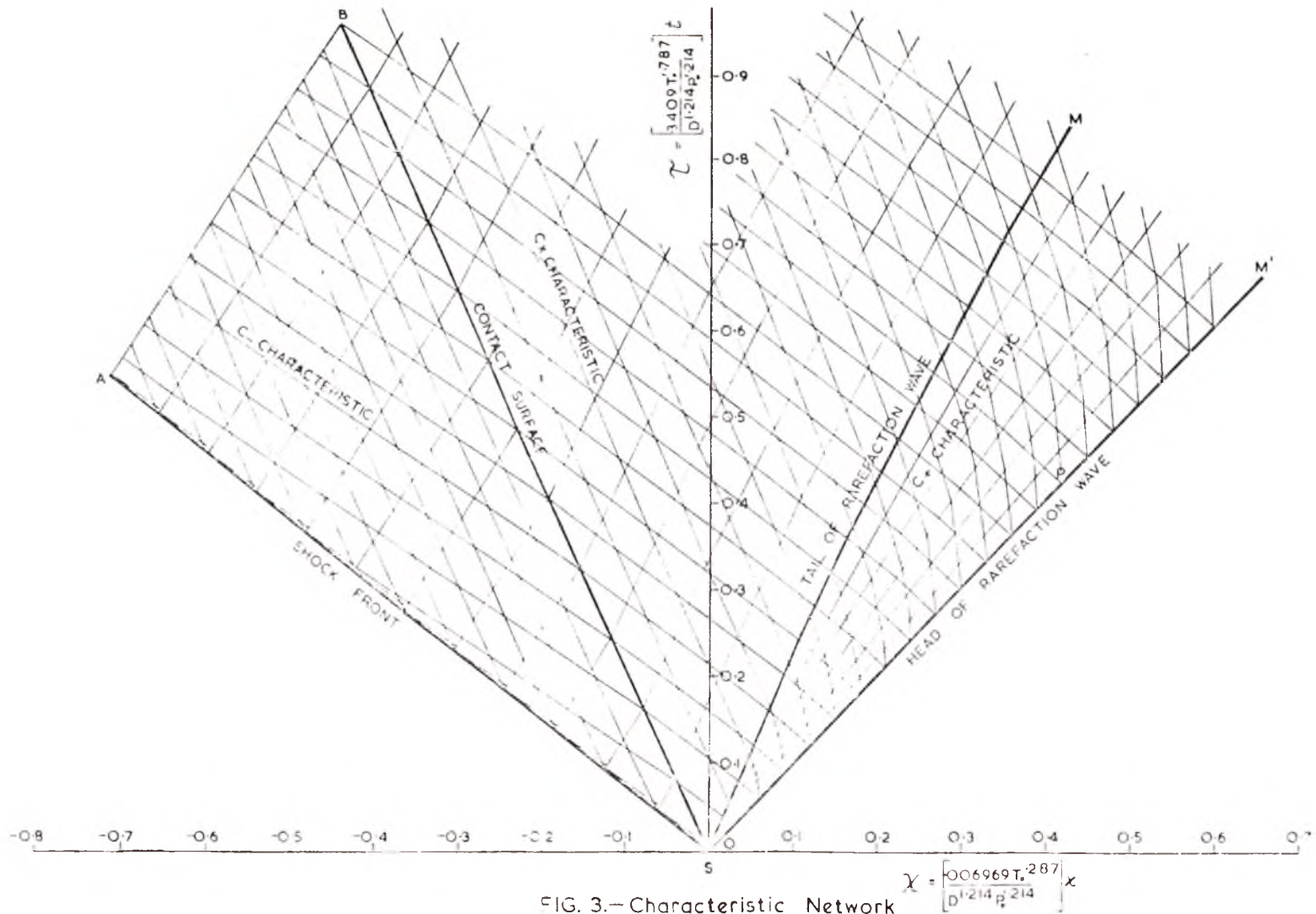


FIG. 3.—Characteristic Network for Pressure Ratio 4:1.

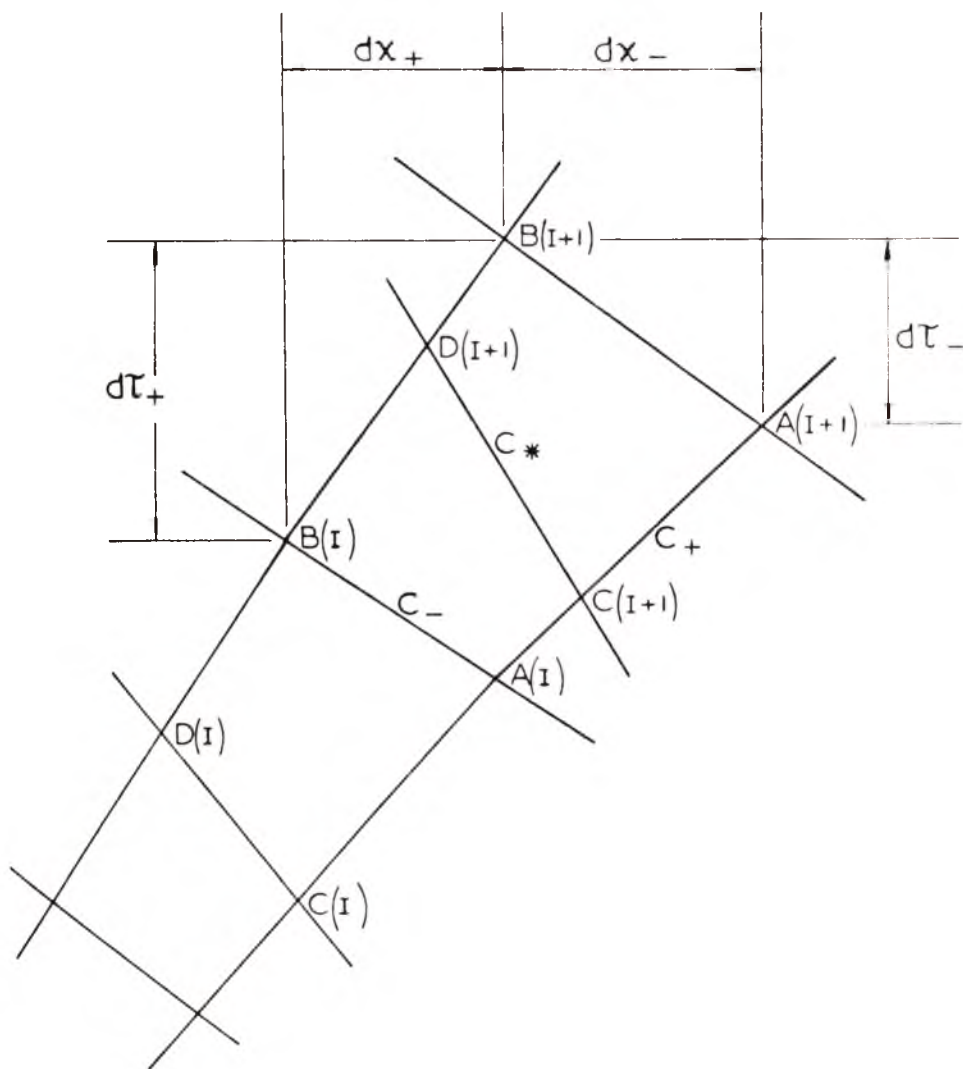


FIG. 4.—Typical Element between Contact Surface and Head of Rarefaction Wave.

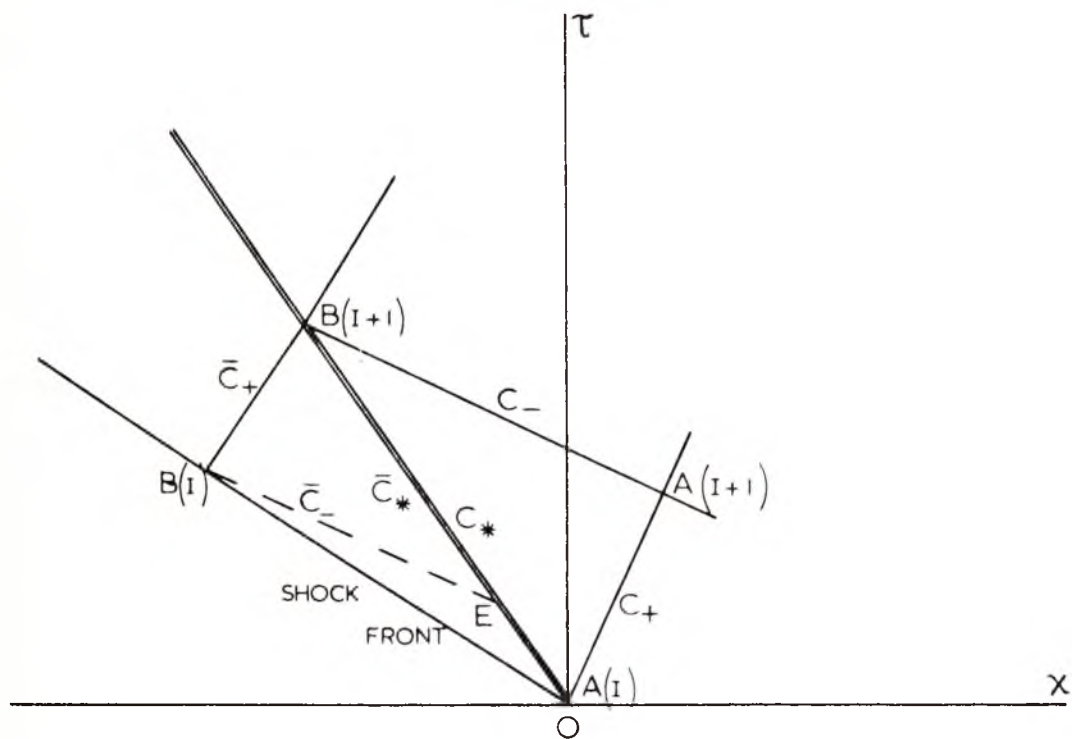


FIG. 5.—Corner Element between Shock Front and Contact Surface.

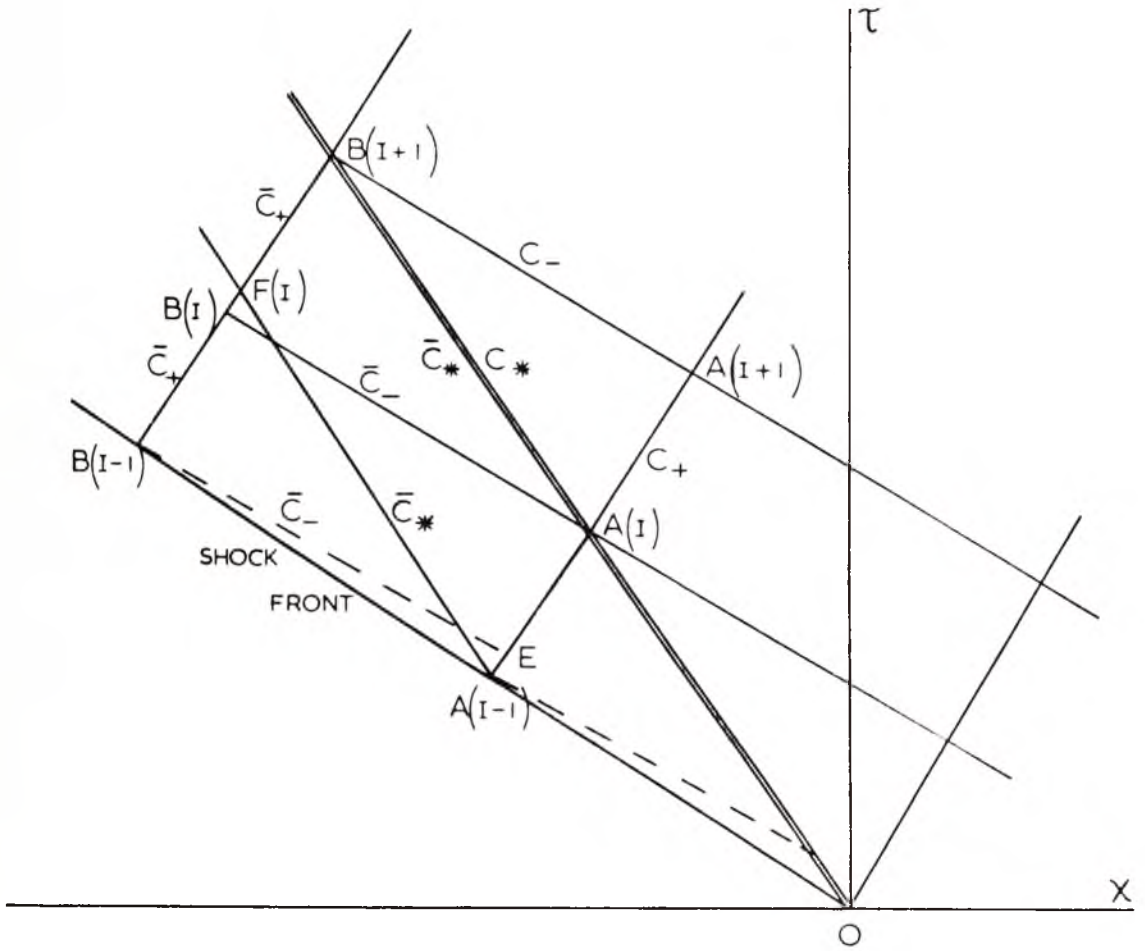


FIG. 6.—Elements on Column 2 between Shock Front and Contact Surface.

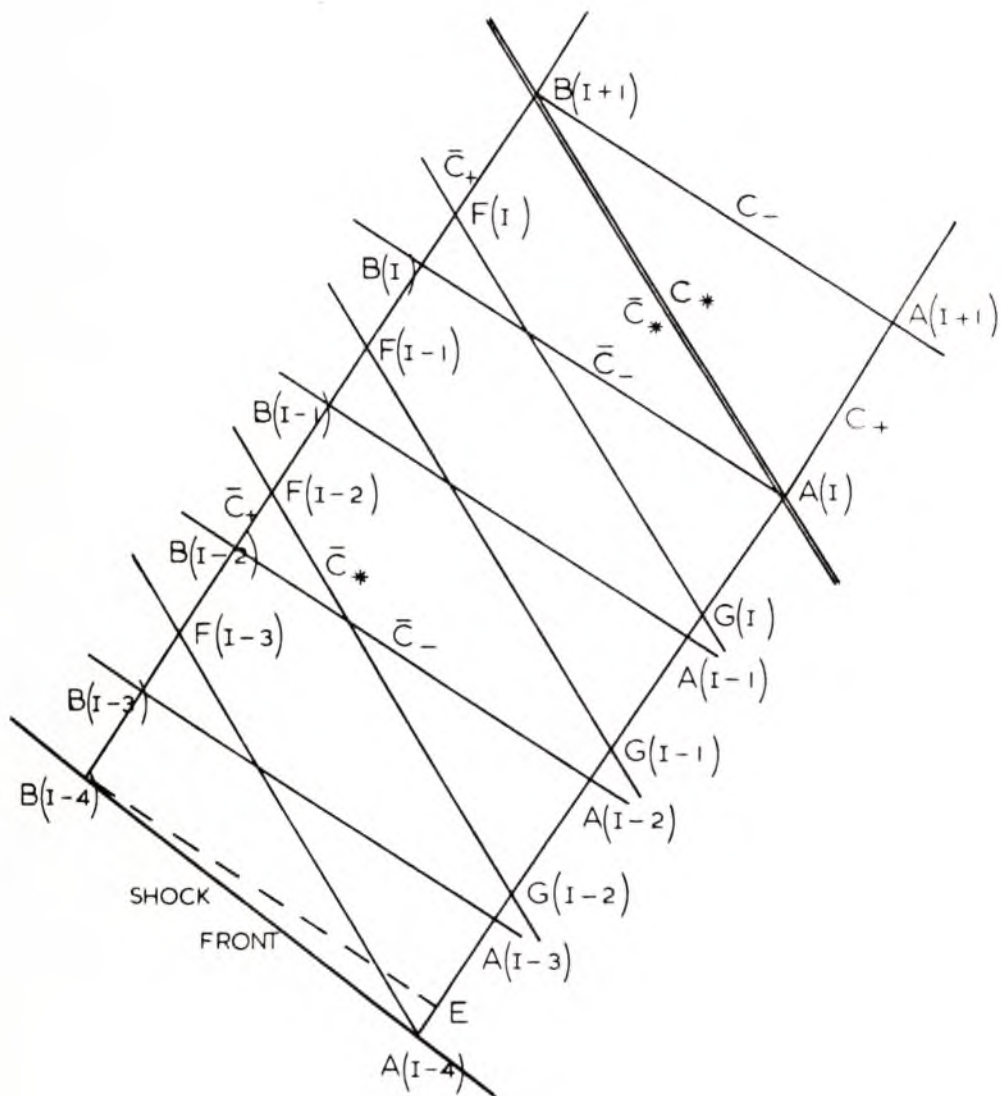


FIG. 7.—Elements on Typical Column between Shock Front and Contact Surface.

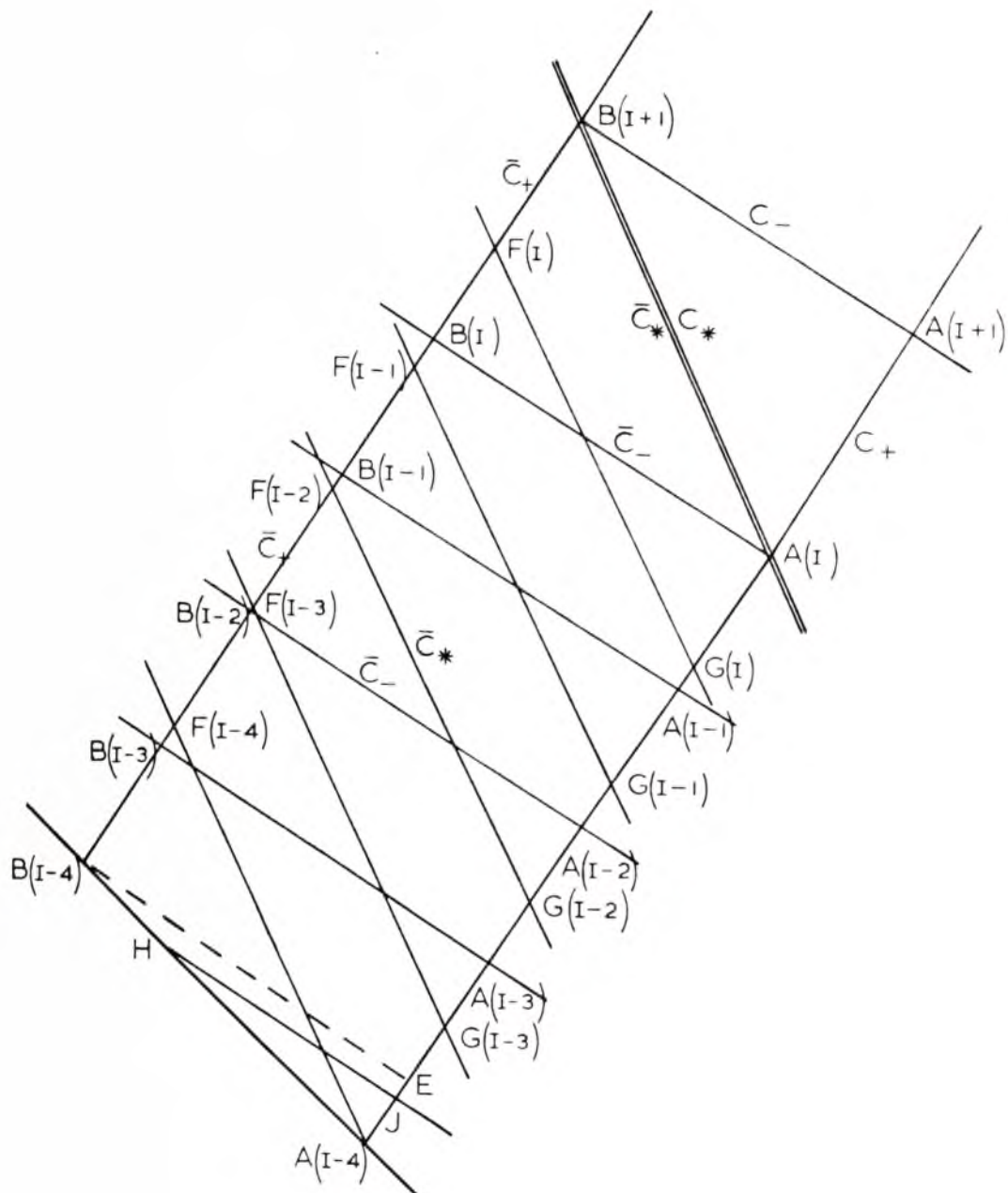


FIG. 8.—Column in which a Gas Particle has Overrun the Shock Front.

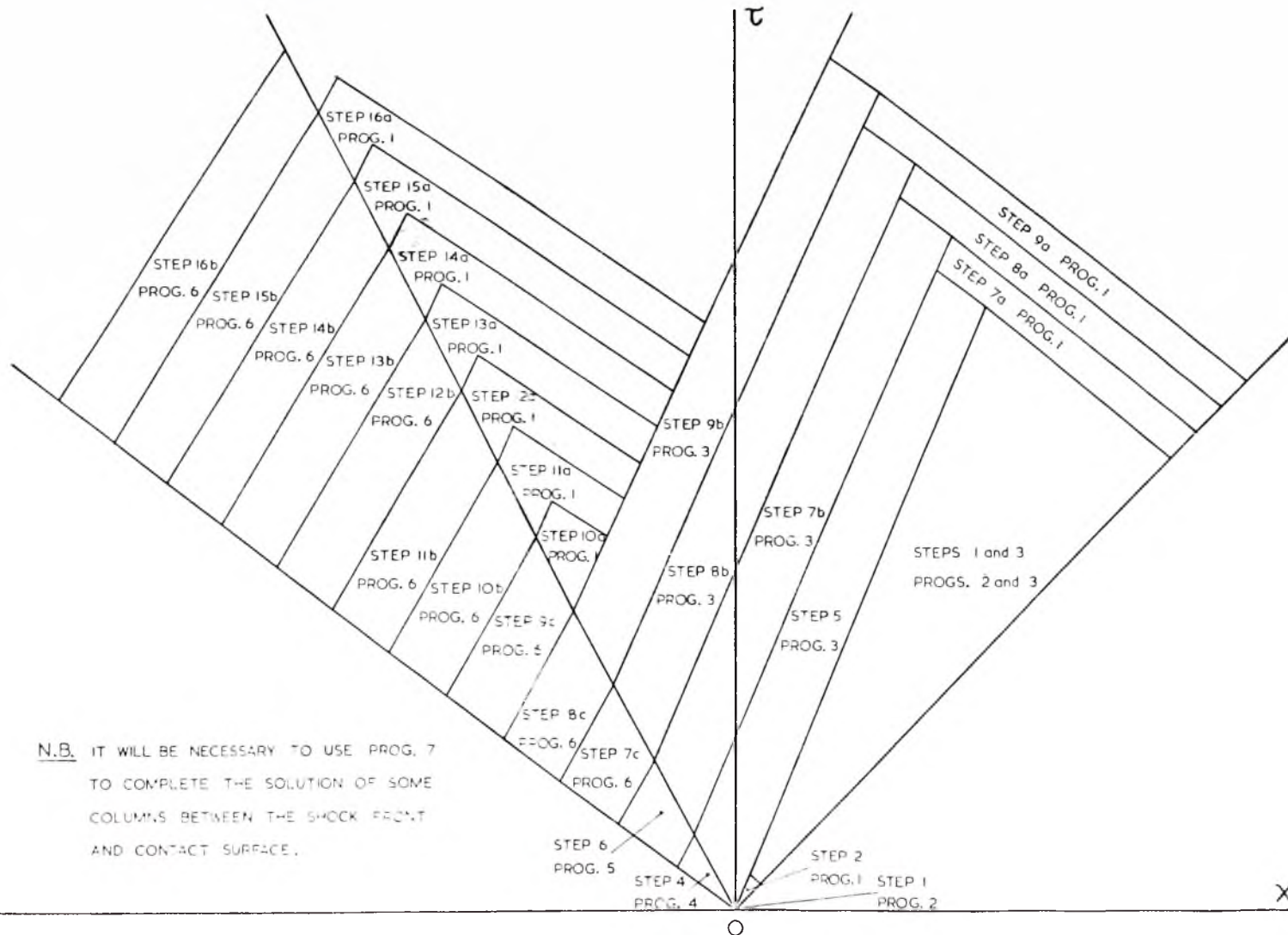


FIG. 9.—Procedure for Computing the Characteristic Network.